

DOI: 10.24425/amm.2019.130092

P. DROŹDŹ\*#

## THE INFLUENCE OF THE SUPERHEAT TEMPERATURE ON THE SLAB STRUCTURE IN THE CONTINUOUS STEEL CASTING PROCESS

The temperature of liquid steel for continuous casting determines the casting speed and cooling conditions. The failure to meet the required casting process parameters may result in obtaining slabs of inconsistent quality. Numerical methods allow for real processes to be modelled. There are professional computer programs on the market, so the results of the simulations allow us to understand the processes that occur during casting and solidification of a slab. The study attempts to evaluate the impact of the superheat temperature on the slab structure based on the industrial operating parameters of the continuous casting machine.

*Keywords:* superheat temperature, continuous casting of steel, ProCAST

### 1. Introduction

Many factors influence the macrostructure obtained in continuously cast steel strands. The relevant factors include the liquid steel superheat temperature, strand geometry, cooling rate and the steel chemical composition. Usually, cast strands have a fine equiaxed grain zone near the surface, called the chilled grain zone, which forms during a fast crystallisation start. Depending on the casting parameters, from the chilled grain zone columnar dendrites grow towards the centre of the cast strand, and equiaxed dendrites form in its central part. The central area can combine columnar and equiaxed dendrites. When the superheat temperature is very high, the equiaxed grain zone may not occur, so the macrostructure comprises entirely columnar dendrites. When the superheat is very low, the slab may solidify with the equiaxed dendrite zone only [1-3]. Figure 1 shows a typical steel

slab structure diagram, divided into zones of chilled, columnar and equiaxed grains.

Based on numerical calculations in the ProCAST software, this paper determines the influence of the superheat temperature on the size of crystals and the type of zone forming in a continuously cast slab. The computations allowed us to indicate differences in the structure of a slab cast at various superheat temperatures, while maintaining industrial cooling conditions during the operation of the continuous caster.

### 2. Characteristics of the continuous steel casting process parameters

The superheat temperature may be distinguished amongst the numerous parameters of the continuous casting process.

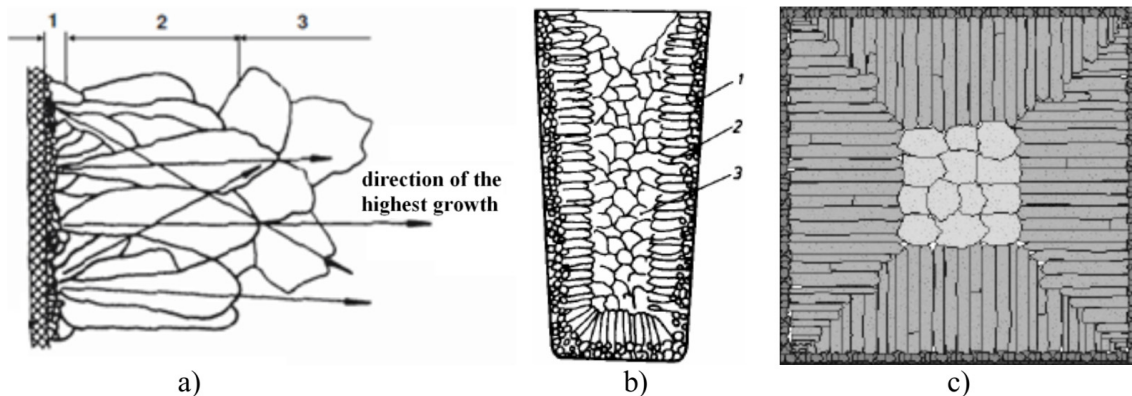


Fig. 1. Steel slab structure diagram. a), b) 1 – chill zone; 2 – columnar zone; 3 – equiaxed zone, c) cross-section perpendicular to the slab axis [4]

\* AGH UNIVERSITY OF SCIENCE AND TECHNOLOGY, FACULTY OF METALS ENGINEERING AND INDUSTRIAL COMPUTER SCIENCE, AL. A. MICKIEWICZA 30, 30-059 KRAKÓW, POLAND

# Corresponding author: pdrozd@agh.edu.pl

It is defined as the difference between the actual temperature of the liquid steel and its liquidus temperature. In industrial conditions, the superheat temperature is between 10 and 50°C [5]. When casting a single heat, the mean temperature of liquid steel in the tundish declines due to heat loss. Therefore, at the same time, the superheat temperature of the steel cast changes, which consequently translates into the quality of the obtained slab. Depending on the chemical composition of the steel cast, in order to ensure the optimal conditions of the solidification process, in industrial practice the maximum strand casting speed declines as the superheat temperature increases. Figure 2 shows the casting temperature impact on the maximum casting speed.

The steel solidification process during continuous casting starts within the mould, which is the primary cooling zone, and next it is continued within the secondary cooling zone, where the slab is cooled with water or air-mist spray. After leaving the chamber, the strand is cooled in the air. The mould, intensely water cooled, gives the required dimensions to the slab cast. During cooling in the mould, a solidified strand layer called the shell forms. Its adequate thickness ensures the continuity of the process without breakouts. The main task of the secondary cooling zone is to continue cooling the strand until it has been fully solidified. The secondary cooling system comprises a few separate zones, in which the strand cooling rate can be controlled. The quality of slabs, in particular of their surface and macrostructure, depends on the operation of the secondary cooling zone.

In this study, a slab with a cross-section of 220 mm × 1600 mm, cast on an arc-shaped continuous caster with a radius of 10500 mm, characterised with a metallurgical length of 23296 mm, was investigated. The strand length to the straightening point was 18103 mm, whereas to the exit from the secondary cooling chamber it was 18438 mm. The mould was cooled at a constant cooling rate, independent of the casting speed. The

secondary cooling was divided into 7 zones, and their cooling rate depended on the casting speed. In addition, the secondary cooling rate, by selecting an appropriate cooling schedule, depended on the steel grade and, therefore, on the carbon and alloy addition contents. Table 1 shows the lengths of the slab cooling zones.

TABLE 1

Strand cooling lengths in individual zones in the process of continuous casting

Cooling zone	Zone length, mm
Mould	800
1 <sup>st</sup> zone	295
2 <sup>nd</sup> zone	1183
3 <sup>rd</sup> zone	1835
4 <sup>th</sup> zone	3687
5 <sup>th</sup> zone	4151
6 <sup>th</sup> zone	4158
7 <sup>th</sup> zone	3345
Air cooling zone	6700

To simplify the calculation process of the numerical simulation, the following assumption were made on the heat transfer characteristics and industrial conditions:

1. Heat transfer along the casting direction is ignored as it occurs much less in comparison to the heat transfer in the direction along the cross-sectional during the continuous casting process of slabs.
2. The effect of the fluid flow of molten steel on the internal heat transfer and structure is ignored during the calculations.
3. Given that there is uniform heat transfer in each part of secondary cooling zone, the heat exchange of the slab in the secondary cooling zone can be described by the heat transfer coefficient.

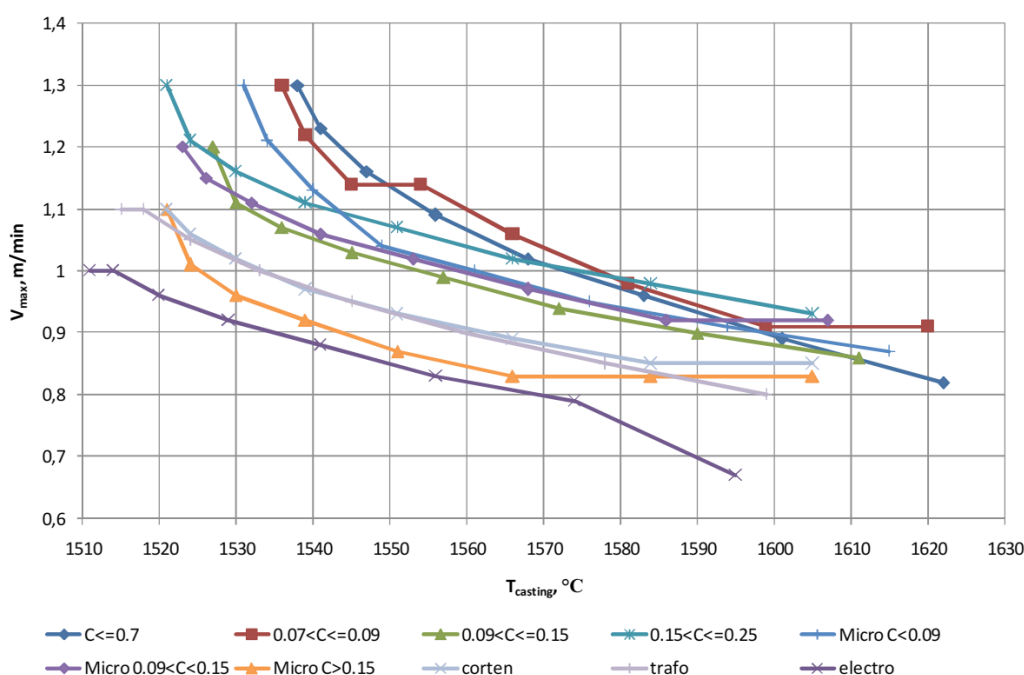


Fig. 2. Casting temperature impact on the maximum casting speed

For the purpose of numerical computing, heat transfer coefficients  $\alpha$  need to be determined, and their values vary depending on the cooling method. The primary cooling takes place within the mould. The secondary cooling is performed with nozzles, through which either water or air-mist flows. The density of heat flux exchanged between the strand and the coolant in the area of the water stream impact is heterogeneous and, therefore, in many cases empirical dependences are assumed for computing. They take into account the most important parameters determining the cooling intensity, arising from the nozzle design, cooling water stream density, its pressure and speed. The heat flux densities, and there by the heat transfer coefficients, depend on the strand surface temperature and the cooling water temperature. The distance of the cooling nozzle outlet to the strand surface is an important factor [6-7]. In the actual continuous casting process, depending on the cooling intensity, individual cooling zones may be characterised by a diversified heat transfer value  $\alpha_{\text{spray}}$  expressed in  $\text{W}/\text{m}^2/\text{K}$  calculated on the basis of the simplified formula (1) [8]:

$$\alpha_{\text{spray}} = 10v + (107 + 0.688v)\dot{V}_{\text{spray}} \quad (1)$$

where:

$v$  – water drop speed, m/s,

$\dot{V}_{\text{spray}}$  – water stream density,  $\text{m}^3/\text{s}/\text{m}^2$ .

This formula allows the heat transfer coefficients to be estimated, not knowing the surface temperature. The water stream density  $\dot{V}_{\text{spray}}$ , and the speed of water drops  $v$  falling onto the strand surface cooled remain to be estimated. The water stream density was calculated knowing the secondary cooling zone area and the water flow rate on the basis of the formula (2):

$$\dot{V}_{\text{spray}} = \frac{V}{S_{\text{zone}}} \quad (2)$$

where:

$V$  – water flow rate,  $\text{m}^3/\text{s}$ ,

$S_{\text{zone}}$  – zone area,  $\text{m}^2$ .

The speed of the water drop outflow from a nozzle was calculated knowing the water flow rate and the nozzle cross-section area, on the basis of the formula (3):

$$v = \frac{V}{S_{\text{nozzle}}} \quad (3)$$

where:

$S_{\text{nozzle}}$  – nozzle cross-section area,  $\text{m}^2$ .

Table 2 shows the speed of water drop outflow from a nozzle for the strand casting speed of 0.8 m/min after taking into account the actual water flow rate in each secondary cooling zone and the corresponding values of heat transfer coefficients  $\alpha$ . The heat transfer coefficients for the mould and for the air cool-

ing are taken from the literature. The calculated values will be used as the boundary conditions for modelling the temperature distribution on the strand using the numerical methods in the ProCAST software.

TABLE 2

Mean heat transfer coefficients  $\alpha$  for casting speed  $V = 0.8$  m/min

Cooling zone	Water drop speed $v$ , m/s	Heat transfer coefficients $\alpha$ , $\text{W}/\text{m}^2/\text{K}$
Mould	—	1600
1 <sup>st</sup> zone	21.3	550
2 <sup>nd</sup> zone	20.3	490
3 <sup>rd</sup> zone	23.4	501
4 <sup>th</sup> zone	10.3	213
5 <sup>th</sup> zone	10.8	170
6 <sup>th</sup> zone	9.3	136
7 <sup>th</sup> zone	11.6	145
Air cooling zone	—	85

### 3. Thermal computations of the continuous casting process

The numerical modelling of the continuous casting process is performed with advanced computer programs [9]. In this project, the ProCAST software package was applied, which enabled the finite element method to be used for computing. The influence of casting temperature, while maintaining the other casting parameters constant, was examined. The continuous casting simulation with the ProCAST software resulted in obtaining the temperature distribution on the strand surface, the length of the liquid core and the shell thickness.

The thermal model of the steel continuous casting process for slabs was prepared on the basis of the actual process engineering parameters. To this end, the slab geometry was prepared, taking into account the division into the existing cooling zones. The same steel grade with the chemical composition shown in Table 3 was assigned to all the strand components.

After implementing the steel chemical composition into the ProCAST program, the material data of the steel grade concerned was computed, and then verified and corrected. The material data includes the thermophysical properties, such as: thermal conductivity, density, enthalpy, solid fraction share and the liquidus and solidus temperatures. The specific heat, along with the heat of fusion of the material used in computing, are amongst the more relevant properties. After assigning the appropriate material to each part of the model, along with the verified material data, the boundary conditions and initial conditions specific to a given process were determined. The prepared geometric model with the

TABLE 3

The chemical composition of the steel taken into account in computing

Al, %	C, %	Cr, %	Cu, %	Mn, %	N, %	Ni, %	P, %	S, %	Si, %
0.0282	0.0966	0.0209	0.0222	0.736	0.0053	0.0731	0.0126	0.0105	0.0184

FEM mesh applied, and with the declared boundary and initial conditions, constitutes a complete data set allowing the simulation to be performed. The computation resulted in obtaining the temperature distribution on the whole strand length for the casting speed of 0.8 m/min depending on the casting temperature. Table 4 shows the summary of the simulation results. Figure 3 shows the selected points on the 1/4 of the cross-section of the strand cast – these points were used for plotting the temperature distribution. Figures 4-6 show the temperature distribution at the selected points along the whole strand length versus casting temperature.

TABLE 4

The summary of simulation results in the thermal model for various casting temperatures and casting speed  $V = 0.8$  m/min

$T_{casting}, ^\circ\text{C}$	Total solidification time, s	Liquid core length, mm	Shell thickness under the mould, mm
1535	988	13.18	24
1545	1012	13.50	
1555	1040	13.87	

Steel casting and cooling in the continuous casting process during a single sequence should enable a slab with a consist-

ent quality to be obtained, regardless of the variable process parameters. The slab should feature similar values as regards the length of the liquid core, shell thickness and temperature distribution along the whole strand length. These properties are related to the design parameters of the continuous caster, and maintaining them at an appropriate level ensures the casting process is failure free. If too thin, the shell under the mould may result in a breakout and spillage of liquid steel onto the rolls. The strand should fully solidify before shearing. On the other hand, the length of the liquid core should not be shorter than the strand length upstream the straightening point, and when the soft reduction system is applied, this length should be closely related to this system. Numerical computing in the thermal model for the selected steel grade, taking into account the actual process parameters, shows certain variations in the results as the casting temperature changes. No variations in computing the shell thickness under the mould versus casting temperature were observed. The computation revealed that when the casting temperature increased while maintaining the same cooling intensity within the secondary cooling zone and the casting speed, the liquid core length slightly changed, which was directly related to various temperatures in the strand centre along the strand for various

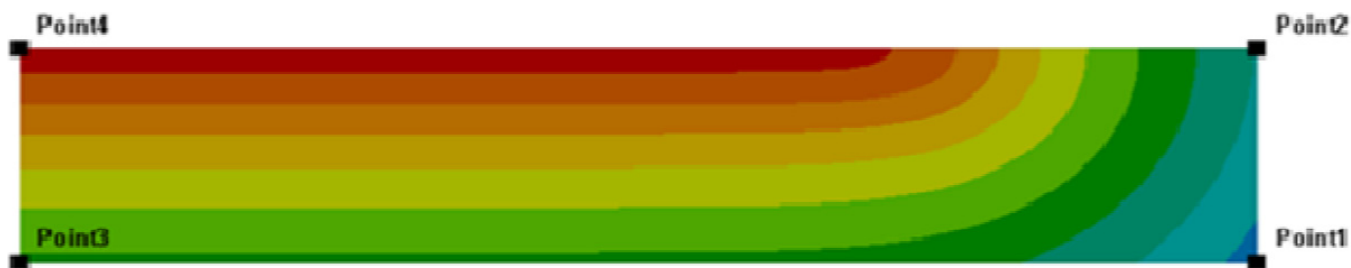


Fig. 3. Selected points at 1/4 of the strand cross-section. Point 1 – slab corner, Point 2 – centre of the slab narrow side, Point 3 – centre of the wide side, Point 4 – slab centre

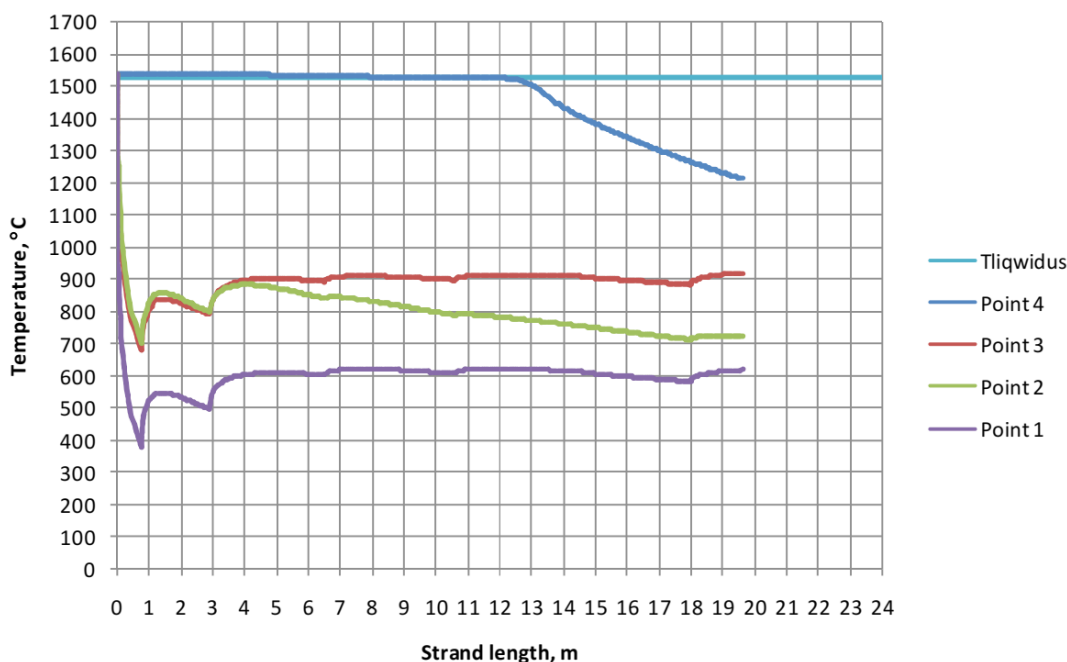


Fig. 4. The temperature distribution at the selected points along the whole strand length for the casting temperature  $T_{casting} = 1535^\circ\text{C}$

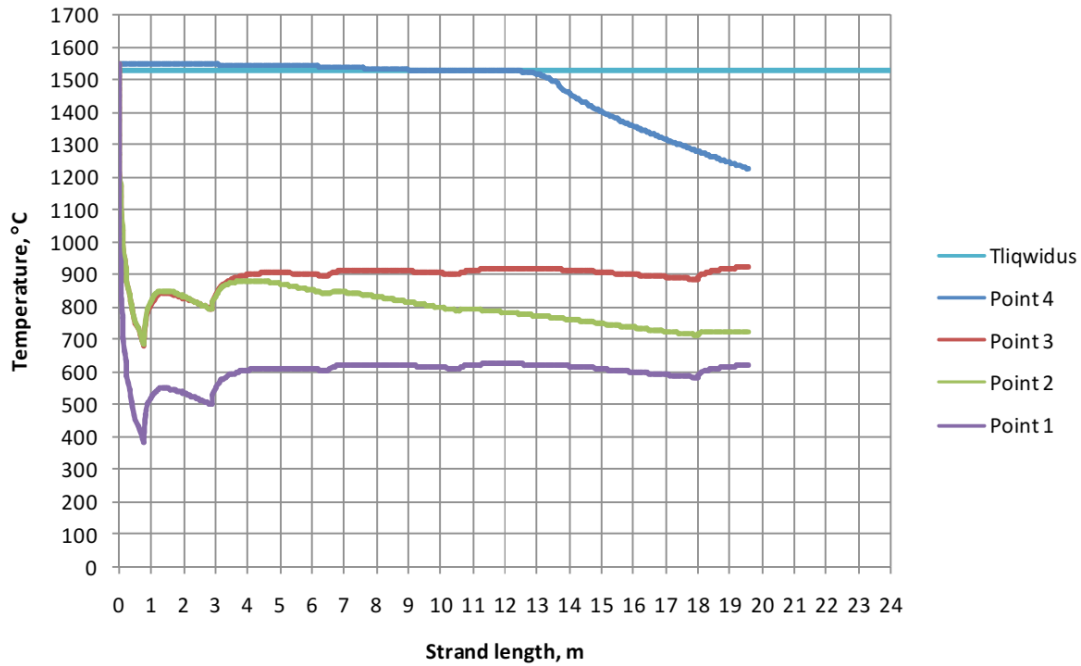


Fig. 5. The temperature distribution at the selected points along the whole strand length for the casting temperature  $T_{casting} = 1545^{\circ}\text{C}$

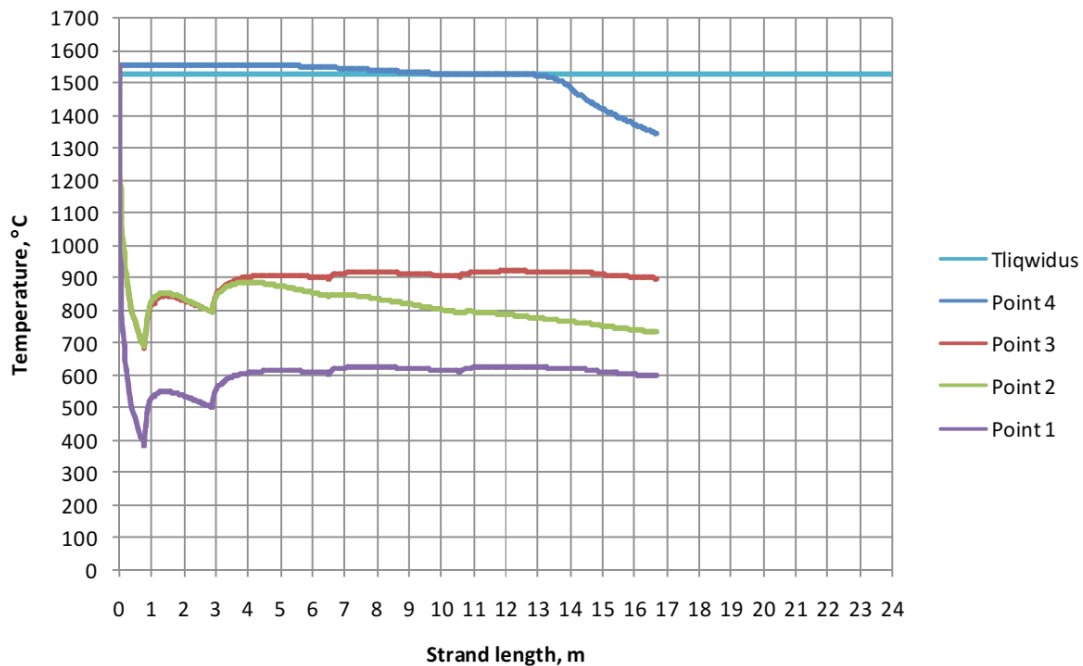


Fig. 6. The temperature distribution at the selected points along the whole strand length for the casting temperature  $T_{casting} = 1555^{\circ}\text{C}$

casting temperatures. An increase in the superheat temperature by  $20^{\circ}\text{C}$  extended the length of the liquid core by about 0.69 m. The strand surface features a similar temperature regardless of the casting speed, which may indicate that the correct casting parameters were selected in the actual process.

#### 4. Modelling the cast strand structure

Attempts to model the processes of slab structure formation, including the nucleation and grain growth, are available in the

literature [10-13]. Numerical models look into the issue of heat flow in the scale of the whole strand, whereas the nucleation and grain growth in the micro scale. Unfortunately, in some models, the columnar zone boundaries and the relationships between the length and the cross-section area of grains cannot be determined. The CAFE model, which is now available as a ProCAST software module, was used to describe the primary phase nucleation and grain growth. This model utilises cellular automata (CA). The cellular automata method enables the grain nucleation on the strand surface and within its volume to be simulated as well as the growth of individual primary phase grains to be examined.



The modelling provides the history of changes in the interface position, and the determination of grain boundaries after the completion of the strand solidification. The CA method computing is coupled with the simulation of the strand temperature field. The nucleation at the strand surface and within its volume is heterogeneous with a random distribution of nuclei. It is assumed that the dependence of the quantity of active nuclei on undercooling is described by the Gauss normal distribution function with the mean  $\Delta T_\mu$  and the standard deviation  $\Delta T_s$  [14]. The values of surface and volumetric densities of nuclei assumed in the modelling, and the Gauss function parameters used in the model, are shown in Table 5.

TABLE 5

Nucleation parameters assumed in the modelling

VOLUME NUCLEATION	
Average undercooling, $\Delta T_\mu$	6
Standard deviation, $\Delta T_s$	0.5
Maximum number of nuclei, $N_{max}$ , $m^{-2}$	$5.0 \times 10^9$
SURFACE NUCLEATION	
Average undercooling, $\Delta T_\mu$	10
Standard deviation, $\Delta T_s$	0.5
Maximum number of nuclei, $G_{max}$ , $m^{-3}$	$5.0 \times 10^9$

The cross-section slab structure resulting from the simulation with cellular automata is shown in Figure 7. A narrow equiaxed chill zone is located at the slab surface. In the cases investigated, the columnar zone in the central part of the slab is

virtually non-existent. The equiaxed zone prevails in the whole cross-section. Table 6 shows a set of parameters characterising the structure resulting from the numerical computing. An increase in the casting temperature significantly influences obtaining a coarse structure of the slab. When the superheat temperature increased by  $20^\circ C$ , an increase in the mean grain area of 24.25% was observed. A similar structure may exist in cast strands. The cross-section slab structure resulting from the industrial process is shown in Figure 8.

TABLE 6

A set of parameters characterising the structure resulting from the numerical computing

$T_{casting}$ , $^\circ C$	Number of grains	Grain surface, $mm^2$			Mean radius of a grain, mm
		Mean	Min	Max	
1535	107886	0.6008	0.36	51.4800	0.52586
1545	97943	0.6617	0.36	65.1602	0.55299
1555	86740	0.7465	0.36	115.5601	0.58718

## 5. Conclusion

The results of the modelling of the cast strand structure obtained with the CAFE method may accurately reproduce the actual structure of slabs produced by continuous casting. However, they do not allow some defects, e.g. axial porosity, to be forecast. In accordance with the results of modelling, the solidification process of a slab with a cross-section of  $220 \times 1600$  mm,

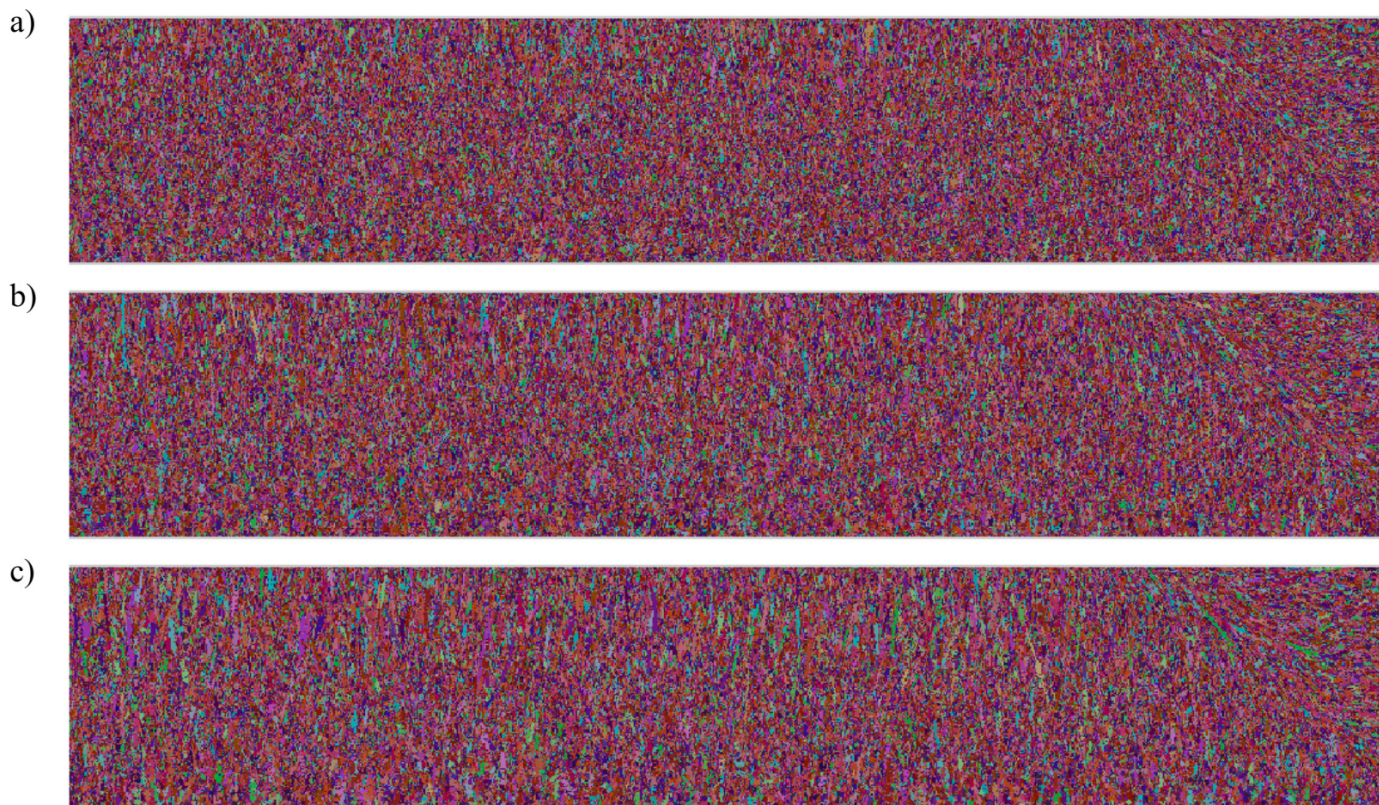


Fig. 7. Results of modelling the primary grain structure in the cross-section of a steel strand with dimensions of  $220 \times 1600$  mm for various casting temperatures: a)  $T_{casting} = 1535^\circ C$ , b)  $T_{casting} = 1545^\circ C$ , c)  $T_{casting} = 1555^\circ C$



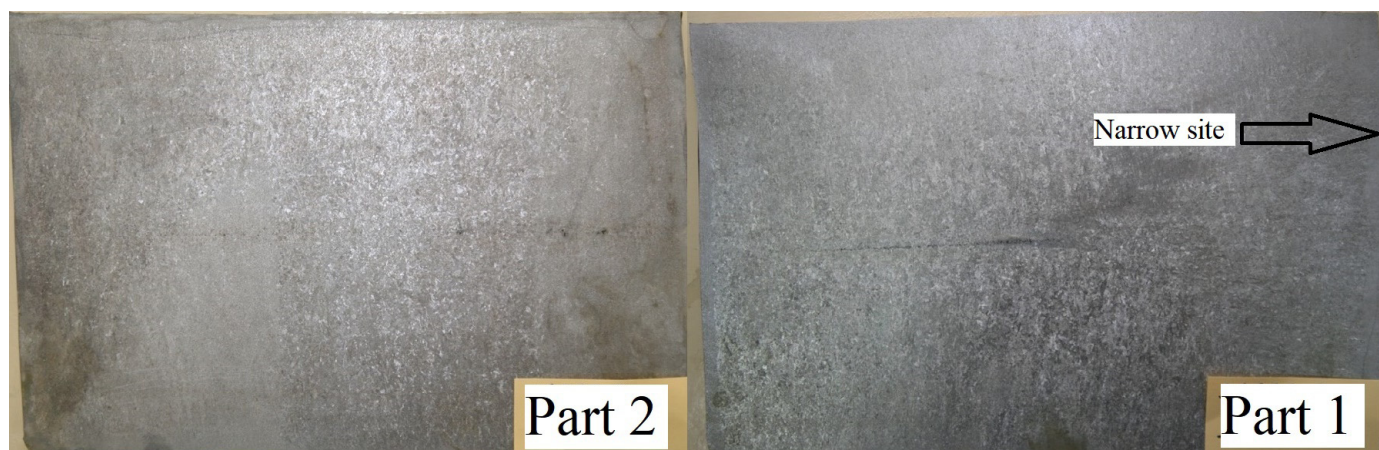


Fig. 8. Results of the primary grain structure in the  $\frac{1}{2}$  of cross-section of a steel strand with dimensions of  $220 \times 1280$  mm obtained during industrial conditions

a diversified structure was obtained subject to the superheat temperature. The columnar zone in the central part of the slab is practically non-existent. An increase in the casting temperature while maintaining a constant cooling rate within the primary and the secondary cooling zones affects the size of the forming primary grains in the slab. When the superheat temperature increased by  $20^{\circ}\text{C}$ , an increase in the mean grain area of 24.25% was observed. A change in the casting temperature taking into account the industrial conditions of cooling results in obtaining a liquid core in the cast strand with various lengths, whereas variations in the temperature distribution at the strand surface are insignificant.

#### Acknowledgements

The study was funded by the Ministry of Science and Higher Education as a statutory work of AGH-UST No 11.11.110 293.

#### REFERENCES

- [1] D.J. Hurtuk, A.A. Tzavaras, Solidification Structures and Continuous Casting of Steel Revisited, *The Journal of The Minerals, Metals & Materials Society* **34**, 2, 40-45(1982).
- [2] T. Pikkarainen, V. Vuorenmaa, I. Rentola, M. Leinonen, D. Porter, Effect of superheat on macrostructure and macrosegregation in continuous cast low-alloy steel slabs. 4th International Conference on Advances in Solidification Processes (ICASP-4), *Materials Science and Engineering* **117**, (2016).
- [3] Liang Bai, Bo Wang, Honggang Zhong, Jie Ni, Qijie Zhai, Jieyu Zhang, Experimental and Numerical Simulations of the Solidification Process in Continuous Casting of Slab, *Metals* **6**, 53 (2016).
- [4] Z. Kudliński, *Technologie odlewania stali*, Wydawnictwo Politechniki Śląskiej, Gliwice, 2006.
- [5] P. Hughes-Narborough, Dynamic Superheat determination in the continuous casting of steel. VIII International Conference on Continuous Casting Of Steel. Technology, Modelling, Defects of CCS ingots, Quality requirements, Conference Proceedings, Krynica, 2018.
- [6] K. Milkowska-Piszczek, J. Falkus, Calculation of the boundary conditions in the continuous casting of steel process, *Metalurgija* **53**, 4, 571-573 (2014).
- [7] K. Milkowska-Piszczek, M. Rywotycki, J. Falkus, K. Konopka, A comparison of models describing heat transfer in the primary cooling zone of a continuous casting machine, *Archives of Metallurgy and Materials* **60**, 1, 239-244 (2015).
- [8] A. Buczek, A. Burbelko, P. Drożdż, M. Dziarmagowski, J. Falkus, M. Karbowniczek, Tomasz Kargul, K. Miłkowska-Piszczek, M. Rywotycki, K. Sołek, W. Ślęzak, T. Telejko, L. Trębacz, E. Wielgosz, *Modelowanie procesu ciągłego odlewania stali – monografia*, Radom 2012.
- [9] B. Thomas, Modeling of the Continuous Casting of Steel-Past, Present and Future, *Electric Furnace Conference Proceedings, ISS* **59**, 3-30 (2001).
- [10] A. Burbelko, J. Falkus, W. Kapturkiewicz, K. Sołek, P. Drożdż, M. Wróbel, Modeling of the grain structure formation in the steel continuous ingot by CAFE method, *Archives of Metallurgy and Materials* **57**, 1, 379-384 (2012).
- [11] M. Rappaz, Ch.-A. Gandin, Probabilistic modeling of microstructure formation in solidification process, *Acta Metallurgica et Materialia* **41**, 2, 345-360 (1993).
- [12] Ch.-A. Gandin, M Rappaz, A coupled finite element-cellular automation model for the prediction of dendritic grain structures in solidification processes, *Acta Metallurgica et Materialia* **42**, 7, 2233-2246 (1994).
- [13] Ch.-A. Gandin, J.-L. Desbiolles, M. Rappaz, Ph. Thevoz, A three-dimensional cellular automation – finite element model for the prediction of solidification grain structures, *Metallurgical and Materials Transactions A* **30A**, 3153-3165 (1999).
- [14] Ph. Thevoz, J.L. Desbiolles, M. Rappaz, Modeling of Equiaxed Microstructure Formation in Castings, *Metallurgical and Materials Transactions A* **20A**, 311-316 (1989).